



## The tale of upper and lower bainite: A computational analysis of concurrent C-diffusion and precipitation

P. Retzl<sup>a,b,\*</sup>, E. Kozeschnik<sup>a</sup>

<sup>a</sup> TU Wien, Institute of Material Science and Technology, Getreidemarkt 9, 1060 Wien, Austria

<sup>b</sup> MatCalc Engineering GmbH, Gumpendorferstraße 21, 1060 Wien, Austria

### ARTICLE INFO

#### Keywords:

Upper bainite  
Lower bainite  
Carbide precipitation  
Carbon partitioning  
Bainite transformation

### ABSTRACT

Carbon partitioning in bainite is a central mechanism controlling this transformation. Depending on whether C atoms form precipitates in the ferrite platelets or remain dissolved in a solid solution, the resulting microstructure is denoted as either lower or upper bainite. In the present analysis, a simulation study is conducted with long-range diffusion of C and simultaneous precipitation of carbides. The computational analysis suggests that carbides always form within the ferritic subunits before carbon redistribution into the surrounding austenite commences, independent of temperature. Since these carbides can rapidly dissolve again at higher bainite transformation temperatures, they are commonly not experimentally observed in upper bainite. At lower temperatures, carbide re-dissolution takes significantly more time, and carbides are, therefore, commonly identified, with the corresponding microstructure denoted as lower-bainite. Since carbides shall always form in the ferrite platelets, a classification of upper and lower bainite based on the existence of carbides should be reconsidered.

Bainite forms by the nucleation of ferritic subunits in austenite and their subsequent growth. The subunits can nucleate either at grain boundaries or autocatalytically at other subunits. An aggregate of subunits with the same crystallographic orientation is called a sheaf. Ferritic subunits grow via a displacive mechanism, i.e., with the speed of sound after their nucleation [1]. Therefore, they are supersaturated in carbon since the solubility of carbon is much lower in ferrite than in austenite. If the excess carbon diffuses into the surrounding austenite before carbides form within the ferritic subunits, the common classification of the resulting microstructure is upper bainite. Otherwise, when carbide precipitates are observed within the ferrite, the microstructure is referred to as lower bainite [2,3]. The carbon, which is ejected by the ferritic subunits, enriches the surrounding austenite, which can then decompose into ferrite and cementite. If carbide formation in austenite is retarded by alloying elements, such as Si or Al, carbide-free bainite is formed, in which the ferritic subunits are surrounded by austenite films [2,4].

Regardless of the assumed mechanism leading to its formation, the presently applied distinction between upper and lower bainite is mostly related to the presence of carbides in the ferritic subunits [5–9].

To predict the type of bainitic microstructure that forms at a given temperature, models have been developed that compare the time

required for the decarburization of the ferritic plates with the time necessary to form a certain amount of carbides within the platelets [10, 11]. These models can predict the transition temperature from upper to lower bainite in a way that achieves a reasonable agreement with the experimental data. However, there are still some discrepancies between simulation and experiment, the cause of which may lie in different aspects of the standard approach to upper and lower bainite. To define a transition temperature from upper to lower bainite (the so-called lower bainite start temperature), the assumption of a limiting carbide phase fraction in the ferritic bainite is necessary since a minimal number of carbides may always form. It seems difficult, though, to pinpoint the exact amount of cementite required to label a bainitic microstructure as lower bainite. In contrast to the models described in references [10,11], the simulation approach presented in the next section couples the C-diffusion between austenite and ferrite directly with the precipitation kinetics. This is a crucial feature, as both processes are strongly coupled and occur as competing microstructural processes.

To describe the mechanisms that govern the formation of a bainitic microstructure, a 1-D cell diffusion simulation is set up with coupled precipitation kinetics calculations. This simulation is performed with the thermokinetic software package MatCalc, version 6.04.0140 [12]. Applications of this software to precipitation kinetics simulations have

\* Corresponding author.

E-mail address: [philipp.retzl@tuwien.ac.at](mailto:philipp.retzl@tuwien.ac.at) (P. Retzl).

been described in previous studies [13,14]. The applied nucleation and growth models were applied for different cases of tempering of martensite for different carbides and showed good agreement with experimental observations [15–19]. The methodology used in the present study for carbide precipitation in bainite, which also involves the investigation of a carbon supersaturated ferritic matrix, is closely related to the tempering of martensite. The thermodynamic database *mc\_fe.tdb* (v2.060) and the diffusion database *mc\_fe.ddb* (v2.012) are used. The cell-diffusion simulation utilizes a finite differences scheme to calculate transient multi-component diffusion profiles. A detailed description of this simulation aspect and its application to C partitioning in carbide-free bainite is reported in Refs. [20,21].

For the current modeling, it is assumed that the ferritic subunits form rapidly via a displacive transformation mechanism. The implications and experimental evidence for either a displacive or diffusional growth mechanism of bainitic subunits are discussed in detail in reference [6]. At the beginning of the simulation, several simulation cells corresponding to the subunit half-thickness are assigned to the ferritic phase (BCC\_A2). Only a half thickness is considered in the calculations due to symmetric boundary conditions at the left end of the simulation box. The remaining cells are initially assigned to the austenite phase (FCC\_A1). The interface between the two phases remains stationary during the simulation. This method is developed and described in Ref. [21] when simulating the C-redistribution between ferrite and austenite films accompanying the bainite transformation.

The composition and assigned thermodynamic phase of a cell define the chemical potential and diffusional mobility of elements within it. Likewise, microstructural properties that affect diffusion, such as the dislocation density, are assigned according to Ref. [21]. The size of the one-dimensional diffusion simulation box is chosen between 300 and 500 nm. A single cell has a length of 1 nm in our setup, which provides a sufficient spatial resolution while sustaining feasible calculation times. This setup resembles a single isolated subunit in an austenite matrix, i.e., no constraint of carbon diffusion by neighboring subunits. The thickness of the ferritic subunits is calculated on a phenomenological basis according to Ref. [22], which was initially developed by Parker [23]. The subunit thickness,  $d_b$ , based on data of steels with C-contents between 0.095 and 0.5 wt% in a temperature range between 523 and 773 K, is approximated as

$$d_b = 2 \cdot 10^{-7} \cdot \frac{T - 528}{150} [m]. \quad (1)$$

Cementite is chosen as the carbide precipitation phase in the ferritic regions. Although a sequence of metastable carbides can form in a bainitic microstructure, this simplification is made because cementite represents the most common carbide occurring in bainite [3]. Other carbides of interest could easily be implemented into the simulation setup, however, without altering the fundamental findings of the present work. They have, therefore, been omitted for the benefit of straightforward interpretation of the results. Dislocations are selected as the nucleation site for these carbides, and a para-equilibrium approach is used to calculate the nucleus's chemical composition [24].

The dislocation density within the ferritic subunits is calculated with an empirical relation from Retzl et al. [21], which reads as

$$\rho_d = 7 \cdot 10^{15} \cdot \frac{1}{0.28\sqrt{2\pi}} e^{-\frac{1}{2} \left( \frac{T}{300} \right)^2}, \quad (2)$$

with  $T_C$  being the temperature in °C.

The lower the bainite transformation temperature, the more critical becomes the impact of C atoms being trapped at defects. It is essential to consider the trapping of C at dislocations since trapped C atoms are not available for precipitation processes. For example, due to this effect, fresh martensite formed at 200 °C can dissolve up to 0.2 wt% of C in thermodynamic equilibrium [25]. The trapping of C in bainitic ferrite is

experimentally confirmed by X-ray and atom probe measurements [26, 27]. The effect of trapping is incorporated in the present simulations with the approach developed by Svoboda and Fischer et al. [28,29,30]. The main input parameters, i.e., trapping enthalpy,  $\Delta E$ , and coordination number,  $c$ , are used with  $\Delta E = 75,000 - 20 \cdot T$  [J/mol] and  $c = A/T^2$ , with the coefficient  $A = 10^6$ , as suggested by Mayer et al. [31].

The model described in the former section is applied to two bainitic alloys with 0.05 wt% and 0.45 wt% C in the temperature range of 300 to 500 °C. The simulations are run for up to 3000 s. The C-concentrations are chosen because, for high temperatures and low C content, i.e., 0.05 wt %, an upper bainite structure with no carbides in the ferritic subunits can be expected, and, for low temperatures and higher C contents, a lower bainite structure with carbides in the subunits will emerge [11].

Fig. 1 shows the evolution of C concentration (a) and phase fraction of carbides (b) for an alloy with 0.05 wt% C at 500 °C directly after the ferrite subunit has formed. The phase boundary between austenite and ferrite is visible in Fig. 1.a in the C concentration jump at roughly 165 nm distance from the subunit center. According to the standard description in the literature, at this low C concentration, no carbides should form within the subunit since the diffusion of C into the surrounding austenite should be faster than the precipitation of carbides. However, according to our simulations, as shown in Fig. 1.b, a significant amount of carbides forms rapidly after the start of the simulation (~1/1000s). During the simulation, these particles only reach a maximum diameter of 3–4 nm and completely dissolve again after approximately 0.4 s. The precipitates dissolve because the C level in the BCC (ferritic) area decreases due to C diffusion into the austenitic regions and the accompanying destabilization of the carbides. At first glance, it may seem of no great interest that very small carbides form and dissolve again within half a second, but it has a significant impact on the partitioning process of C. The time necessary for C to diffuse out of the subunit increases severely because the carbon, which is bound in the form of carbides, is not readily available for diffusion. Therefore, simple assumptions that consider the evacuation of C from the subunit and carbide precipitation as separate processes underestimate the time that it takes for the C concentration in the ferritic bainite plates to reach equilibrium.

A different behavior occurs if a C content of 0.45 wt% at 300 °C is investigated. Similar to the low-C high-temperature case, carbides form rapidly in the subunit (~0.01 s until the maximum phase fraction is reached). These precipitates bind nearly all C in the ferritic region, and, in combination with the slow diffusion at 300 °C, almost no C redistribution occurs within 3000 s. The evolution of the C profile is shown in Fig. 2.a. The carbides reach a maximum mean diameter of 12 nm, and their phase fraction stays nearly the same throughout the simulation. Only after about 3000 s, as shown in Fig. 2.b, does the carbide volume fraction start to decrease at the edge of the ferrite region. When investigating bainite after 3000 s of transformation, many carbides are still present in the ferritic subunits, thus resembling the lower bainite microstructure. On prolonged aging at this temperature, the carbides will still dissolve. The lower bainite microstructure is thus, in principle, the same as upper bainite. However, it is looked at before sufficient time has passed to dissolve the carbides again and let the C atoms diffuse into the austenite films and blocks.

Since carbides always precipitate during the simulation and a dissolution process takes place in all environments examined, it is essential to know how long this process takes to understand the implications for the microstructure evolution of bainite. Fig. 3 shows the necessary time for the carbide phase fraction to reach a maximum and be reduced to zero for different temperatures and the two investigated C contents. While, for the low C content (0.05 wt %), even at 300 °C, the dissolution process takes place within 200 s, for the higher C content (0.45 wt %), nearly no carbides have dissolved even after 3000 s. Since the bainite transformation process takes some hundreds of seconds at conventional production conditions [32], the commonly and practically observed microstructure under these conditions will generally be

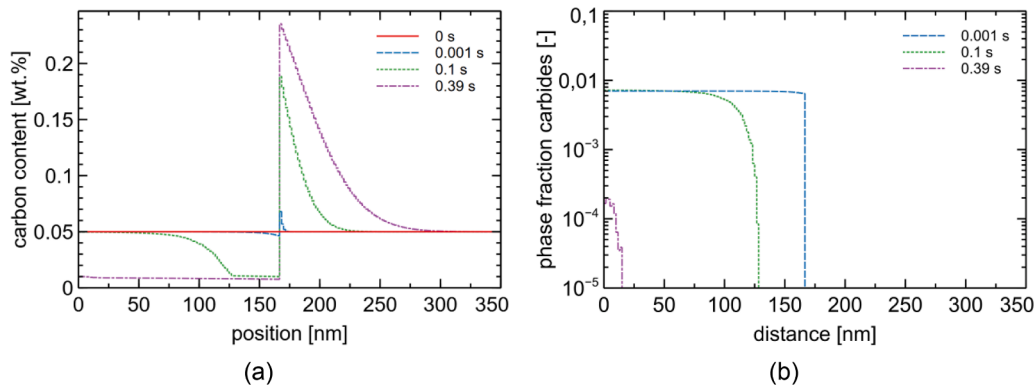


Fig. 1. Precipitation and long-range diffusion simulation at 500 °C with 0.05 wt% C (a) evolution of C concentration profile (b) carbide volume fraction profile.

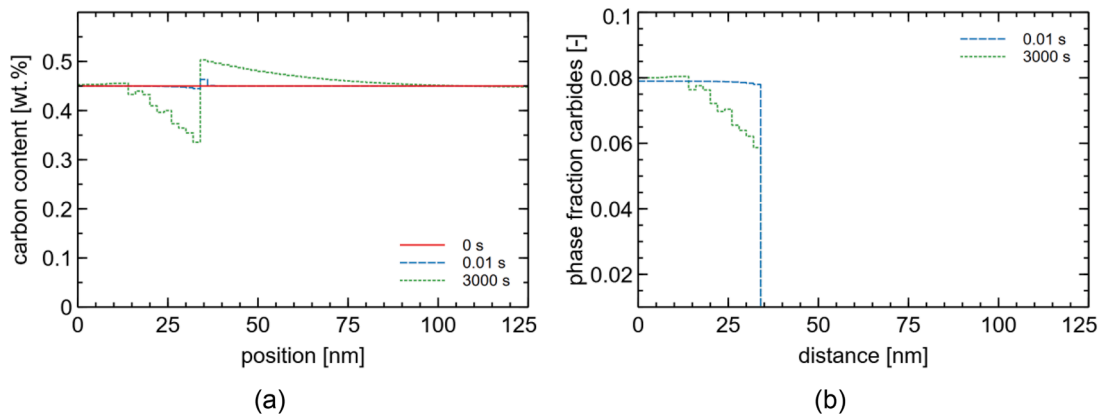


Fig. 2. Simulation at 300 °C with 0.45 wt% C (a) evolution of C concentration profile (b) carbide volume fraction profile.

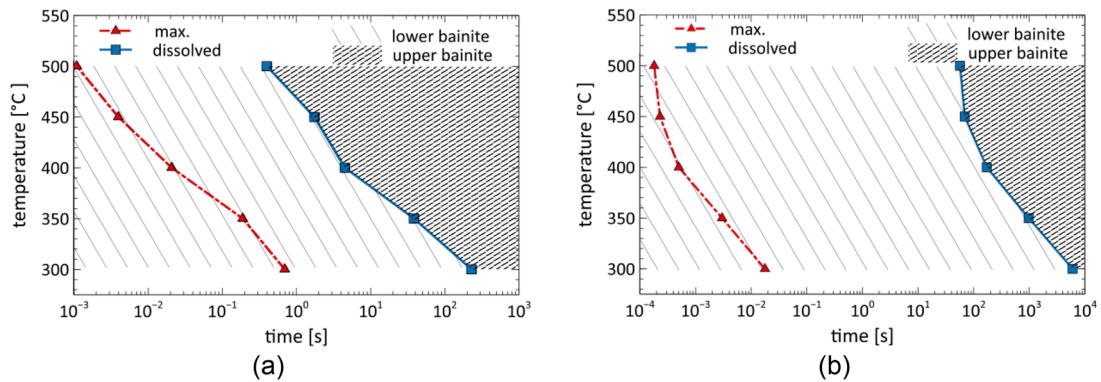


Fig. 3. Simulation results of the presented model. Time until maximum phase fraction of carbides is formed within the ferritic bainite subunits (red triangles) and time until all carbides are dissolved (blue squares) as a function of temperature for C content of 0.05 wt%(a) and 0.45 wt% (b). Differently, shaded areas indicate if upper or lower bainite will be observed.

denoted as lower bainite.

In essence, our simulations suggest that upper and lower bainite share the same formation processes. Subunits always go through the stages of C supersaturation, carbide formation within the subunit, carbon partitioning to the surrounding austenite, and, given enough time, dissolution of the carbides within the subunit. It only takes fractions of a second for low-C alloys at high temperatures to go through this process but several thousand seconds for the high-C and low-temperatures cases. Depending on when an observer looks at the microstructure, either upper or lower bainite is diagnosed. Incorporating metastable transition carbides into the simulation would not change the predicted sequence of initial carbide precipitation followed by their dissolution. These

precipitates form more rapidly than cementite at lower temperatures, which should only amplify the effect of precipitation occurring before complete carbon partitioning, leading to a shift of the maximum phase fraction in Fig. 3 to the left.

Observing the rapid formation and dissolution process of carbides at higher temperatures is challenging due to the short time and small size scale. However, the dissolution of carbides in a high-C low-temperature case could be observed if the bainite is tempered for much longer than necessary for complete transformation. The onset of this dissolution process would manifest itself in the formation of carbide-free zones at the border of a subunit, according to Fig. 2. b. Experimental evidence for the formation of carbide-free zones in subunits has been reported in

Ref. [33].

These carbide-free zones are found in subunits located at the border of sheaves. This corresponds to our simulation setup of a single subunit surrounded only by austenite and no other subunits close to it. An assumption in our modeling approach that could influence its predictive accuracy is the neglect of carbide formation at the ferrite/austenite interface. If a high number of carbides would rapidly form at this interface, this could also lead to carbon depletion around the interface, which could promote the formation of a carbide-free zone, as mentioned above. Although no carbides at the interface have been documented in Ref. [33] this could be the case for other alloys. A case where carbide precipitation is suppressed in austenite and seemingly also at the austenite/ferrite interface, like in Ref. [33], resembles a situation similar to our simulation setup, which does not consider carbide nucleation in the austenite region or directly at the interface.

A model capable of simultaneously describing the long-range diffusion of C and the precipitation of carbides within and around a bainite subunit is used to study the redistribution of C and the concurrent precipitation of carbides in bainitic microstructures. The simulations show that, even at low C concentrations and high temperatures, where the final microstructure is commonly denominated as upper bainite, carbide precipitates form within a subunit shortly after its formation. These carbides dissolve again rapidly, however, due to C diffusion into the surrounding austenite. Since the analysis demonstrates that carbide precipitation always occurs, the denomination of the observed microstructure apparently depends on the particular moment when the microstructure is looked at and, in particular, whether the carbides have had sufficient time to dissolve again. Additionally, if the predictions of the presented approach are correct, the state of a subunit would depend on the time when it formed during the bainite transformation. Subunits formed at the start of the transformation would more often resemble upper bainite. In contrast, subunits formed at the end of the bainite transformation or shortly before quenching to RT would not have sufficient time for carbide dissolution and, therefore, be observed as lower bainite. This implies that the transition from upper to lower bainite is more of a smooth transition than a sudden change in mechanism depending only on temperature and carbon content. This may be one of the reasons why models, as described in Ref. [11], are not capable of predicting the onset of lower bainite formation with high accuracy. However, both the referenced approach and the one described in the present work rely on the assumption that bainite subunits grow through a displacive mechanism, leading to supersaturation in the ferritic areas. If this premise holds true, it would imply a need to revisit the classification of upper and lower bainite, which is currently often solely based on carbide presence or absence.

## Declaration of competing interest

The authors declare that they have no known competing financial interests or personal relationships that could have appeared to influence the work reported in this paper.

## References

- [1] H.K.D.H. Bhadeshia, D.V. Edmonds, *Acta Metall.* 28 (1980) 1265–1273.
- [2] M. Takahashi, H.K.D.H. Bhadeshia, *Mater. Sci. Technol.* 6 (1990) 592–603.
- [3] H.K.D.H. Bhadeshia, *Bainite in Steels*, 3rd ed., 2015.
- [4] L.C. Chang, *Mater. Sci. Eng. A* 368 (2004) 175–182.
- [5] G. Spanos, H.S. Fang, H.I. Aaronson, *Metall. Trans. A* 21 (1990) 1381–1390.
- [6] L.C.D. Fielding, *Mater. Sci. Technol.* 29 (2013) 383–399.
- [7] F.G. Caballero, M.K. Miller, C. Garcia-Mateo, *Mater. Chem. Phys.* 146 (2014) 50–57.
- [8] S.A. Sajjadi, S.M. Zebarjad, *J. Mater. Process. Technol.* 189 (2007) 107–113.
- [9] H. Ohtani, S. Okaguchi, Y. Fujishiro, Y. Ohmori, *Metall. Trans. A* 21 (1990) 877–888.
- [10] M. Azuma, N. Fujita, M. Takahashi, T. Lung, *Mater. Sci. Forum* 45 (2003) 221–228.
- [11] L. Guo, H. Roelofs, M.I. Lembke, H.K.D.H. Bhadeshia, *Mater. Sci. Technol.* 33 (2017) 430–437.
- [12] E. Kozeschnik, *Encycl. Mater. Met. Alloy.* 4 (2021) 521–526.
- [13] R. Radis, E. Kozeschnik, *Model. Simul. Mater. Sci. Eng.* (2012) 20.
- [14] S. Zamberger, M. Pudar, K. Spiradek-Hahn, M. Reischl, E. Kozeschnik, *Int. J. Mater. Res.* 103 (2012) 680–687.
- [15] S. Zamberger, L. Whitmore, S. Krisam, T. Wojcik, E. Kozeschnik, *Model. Simul. Mater. Sci. Eng.* (2015) 23.
- [16] S. Zamberger, T. Wojcik, J. Klarner, G. Klösch, H. Schifferl, E. Kozeschnik, *Steel Res. Int.* 84 (2013) 20–30.
- [17] S.D. Yadav, B. Sonderegger, M. Stracey, C. Poletti, *Mater. Sci. Eng. A* 662 (2016) 330–341.
- [18] T. Zhou, J. Lu, P. Hedström, *Metall. Mater. Trans. A Phys. Metall. Mater. Sci.* 51 (2020) 5077–5087.
- [19] S. Hollner, B. Fournier, J.L. Pendu, T. Cozzika, I. Tournié, J.C. Brachet, A. Pineau, *J. Nucl. Mater.* 405 (2010) 101–108.
- [20] Y.V. Shan, M. Soliman, H. Palkowski, E. Kozeschnik, *Steel Res. Int.* 92 (2021).
- [21] P. Retzl, S. Zamberger, E. Kozeschnik, *Mater. Res. Express* 8 (2021).
- [22] H. Matsuda, H.K.D.H. Bhadeshia, *Proc. R. Soc. A Math. Phys. Eng. Sci.* 460 (2004) 1707–1722.
- [23] S.V. Parker, (1998).
- [24] E. Kozeschnik, H.K.D.H. Bhadeshia, *Mater. Sci. Technol.* 24 (2008) 343–347.
- [25] G. Speich, *Trans Met Soc AIME* 245 (1969) 2553–2564.
- [26] F.G. Caballero, H.K.D.H. Bhadeshia, *Curr. Opin. Solid State Mater. Sci.* 8 (2004) 251–257.
- [27] M. Peet, S.S. Babu, M.K. Miller, H.K.D.H. Bhadeshia, *Scr. Mater.* 50 (2004) 1277–1281.
- [28] J. Svoboda, Y.V. Shan, E. Kozeschnik, F.D. Fischer, *Model. Simul. Mater. Sci. Eng.* 21 (2013) 065012.
- [29] J. Svoboda, F.D. Fischer, *Acta Mater.* 60 (2012) 1211–1220.
- [30] F.D. Fischer, J. Svoboda, E. Kozeschnik, *Model. Simul. Mater. Sci. Eng.* 21 (2013) 025008.
- [31] W. Mayer, S. Sackl, Y.V. Shan, S. Primig, E. Kozeschnik, *Mater. Today Proc.* 2 (2014) S619–S622.
- [32] D. Quidort, Y.J.M. Brechet, *ISIJ Int.* 42 (2002) 1010–1017.
- [33] T. Klein, C. Hofer, M. Lukas, T. Wojcik, R. Schnitzer, M. Galler, G. Ressel, *Materialia* 7 (2019) 100380.